POLITECNICO DI TORINO
Repository ISTITUZIONALE

Propeller Aerodynamics Under Non-Uniform Inflows

Original
Propeller Aerodynamics Under Non-Uniform Inflows / Montagner, S., Zannone, M., Serpieri, J., Cafiero, G.. - 69:(2026), pp. 707-712. (10th CEAS Aerospace Europe Conference and 28th AIDAA International Congress, 2025 Turin (ITA) December 1-4, 2025) [10.21741/9781644904251-125].

Availability:
This version is available at: 11583/3017729 since: 2026-11-10T09:46:29Z

Publisher:
Association of American Publishers

Published
DOI:10.21741/9781644904251-125

Terms of use:

This article is made available under terms and conditions as specified in the corresponding bibliographic description in the repository

Publisher copyright

(Article begins on next page)

18 November 2026

Materials Research Proceedings 69 (2026) 707-712 https://doi.org/10.21741/9781644904251-125

Propeller Aerodynamics Under Non-Uniform Inflows

Sara MONTAGNER[1,a *], Manuel ZANNONE[1,b], Jacopo SERPIERI[1,c] and Gioacchino CAFIERO[1,d]

[1]Department of Mechanical and Aerospace Engineering, Politecnico di Torino, Corso Duca degli Abruzzi 24, Turin, Italy

[a]sara.montagner@polito.it, [b]manuel.zannone@polito.it, [c]jacopo.serpieri@polito.it, [d]gioacchino.cafiero@polito.it

Keywords: UAM, UAVs, Propeller, Non-Uniform Inflow, Aerodynamics

Abstract. Urban Air Mobility (UAM) is highly dependent on Unmanned Aerial Vehicles (UAVs) operating in complex urban environments, where propellers often encounter non-uniform inflows. These conditions can deteriorate the performance and stability of the vehicle, making standard uniform-inflow assumptions unrealistic and even dangerous for the prediction of the performance of UAVs. It is therefore of paramount importance to develop the capability to accurately reproduce in a repeatable manner such complex inflow conditions. This paper presents an experimental investigation of a propeller wake under controlled, non-uniform sheared inflow. Using Particle Image Velocimetry (PIV), the wake of a D=0.3 m propeller was characterized when operating in forward flight conditions. A modular fan array generated both uniform baselines and four linear shear rates. The results show that the sheared inflow creates an asymmetric wake with reduced vorticity magnitude and a radial streamtube expansion. Furthermore, Turbulent Kinetic Energy (TKE), highly localized in uniform flow, becomes significantly more diffused under sheared conditions, indicating altered turbulent mixing. These findings highlight the critical impact of the inflow conditions on the on the wake development.

Introduction

The viability of Urban Air Mobility (UAM) requires a step forward in the deployment of Unmanned Aerial Vehicles (UAVs), especially when operating in complex urban environments. Applications such as logistics and surveillance require low-altitude flight, where UAV propellers inevitably encounter non-uniform inflows, owing to the presence of unstructured environments, buildings and street canyons. These conditions significantly deviate from the ideal, uniform flow assumptions typically employed especially at a preliminary design stage. Operating in such perturbed aerodynamic environments can deteriorate propeller efficiency, induce unsteady loads, and compromise flight stability. Consequently, standard performance models, which assume uniform inflow, are often unrealistic. This discrepancy can lead to the underestimation of energy consumption and control effort required for stable flight, particularly in challenging scenarios like urban delivery, where adverse atmospheric disturbances are common [1].

Despite the clear operational need, many assessments of UAV propulsion systems and aerodynamics still rely on simplified inflow assumptions, potentially leading to overestimation of performance and reliability. Although the detrimental impact of non-uniform inflows is well-recognized, dedicated studies in the literature remain limited, particularly on the experimental side. Much of the available research relies on numerical simulations (CFD) to investigate the aerodynamic performance and forces on propellers subjected to wind fields [2]. Experimental work, in turn, has provided comprehensive force and flow-field datasets for propellers in steady non-axial (yawed) inflow conditions [4]. However, more complex simulations and experimental studies highlight that accurately modeling gust effects is crucial for predicting power consumption, as simplified aerodynamic models fail to capture performance degradation under high gust

Content from this work may be used under the terms of the Creative Commons Attribution 3.0 license. Any further distribution of this work must maintain attribution to the author(s) and the title of the work, journal citation and DOI. Published under license by Materials Research Forum LLC.

intensity [3]. Furthermore, accurately and repeatably simulating complex spat-temporal disturbances, such as the sheared inflows investigated in this work, remains a significant challenge for conventional wind tunnel facilities [3]. To address this gap, the present study takes a first step by experimentally characterizing the wake flow field of a propeller operating under controlled sheared inflow conditions.

Experimental setup

Experiments were performed in the indoor flight arena at Politecnico di Torino. The facility is equipped with a WindShaper modular fan array [5], which comprises an 8 × 6 matrix of modules with individually controllable fans. This setup creates a 2 m × 1.5 m active test section, enabling the generation of both uniform and precisely controlled non-uniform inflow profiles.

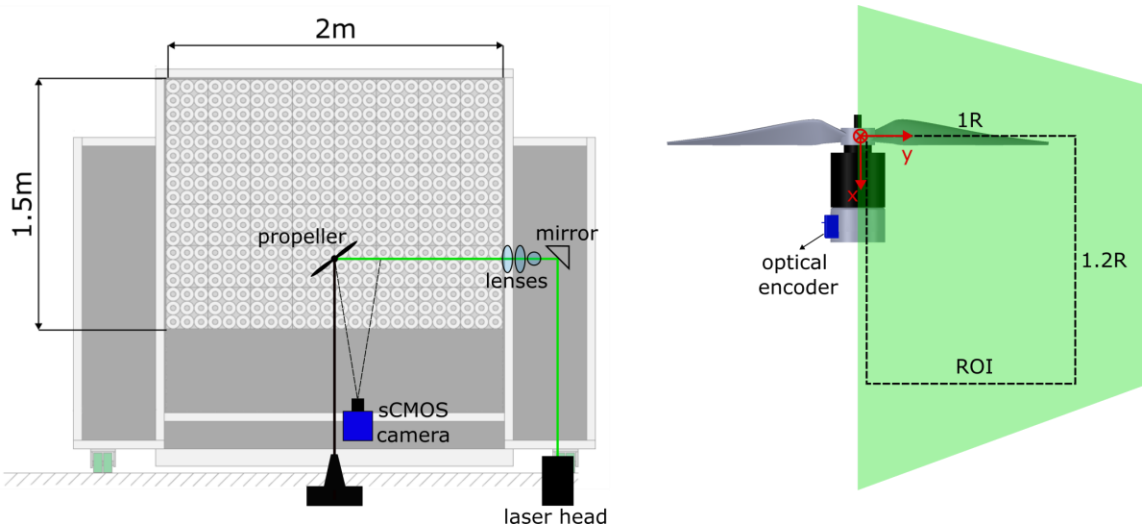


Figure 1: Schematic of the experimental setup.

The propeller used in the experiments was 3D-printed in resin with a diameter of D = 2R = 0.3 m, following the geometry from [6]. It was actuated by a brushless motor and an Electronic Speed Controller (ESC), controlled via an Arduino UNO board. An optical rotary encoder monitored the propeller's rotational speed, which was held constant at 2000 rpm for all tests. The propeller was positioned 1 m downstream from the fan array, with its rotation plane parallel to the fan wall to simulate forward flight. Particle Image Velocimetry (PIV) was employed to characterize the propeller's wake field; a schematic of the setup is shown in Figure 1. The flow was seeded with 1 µm diameter droplets generated by a Laskin nozzle. The region of interest was illuminated by a dual-pulse Nd:YAG laser (200 mJ/pulse) operating at 15 Hz. The laser beam was shaped into a 1 mm thick sheet, and the time separation between pulses was set to Δt =140 µs. PIV images were acquired using a 5.5 MP sCMOS camera (2560 × 2160 pixels) equipped with a 60 mm focal length lens set to $f_{\#}$=11. The imaged area covered approximately 1 R (radial, y) by 1.2 R (streamwise, x) downstream of the propeller, yielding a digital resolution of 13.5 px/mm. For each test case, 2200 image pairs were acquired. Raw images were pre-processed by subtracting the historical minimum to each acquired image in the dataset. Vector fields were computed using the PaIRS software [7] via a multi-step cross-correlation algorithm, using a final interrogation window of 32 × 32 pixels with 75% overlap. This resulted in a final vector spacing of 0.59 mm.

The experimental campaign focused on two primary inflow scenarios: uniform and non-uniform (shear flow). For the uniform inflow case, the advance ratio, defined as $J = U/(nD)$ was systematically varied over the range $0.2 \leq J \leq 0.7$. For the non-uniform cases, the WindShaper generated linear shear flow profiles across the propeller disk (in the y-direction). In these

Materials Research Proceedings 69 (2026) 707-712 https://doi.org/10.21741/9781644904251-125

configurations, the advance ratio, calculated using the velocity at the propeller hub ($y/R = 0$), was varied within the range $0.4 \leq J \leq 0.6$. Four distinct shear intensities were investigated, defined by the tip-to-tip velocity difference (ΔV_k) across the propeller: 1, 1.5, 2, and 3 m/s. These cases are hereafter denoted as SR_1 through SR_4, respectively.

Results

The analysis begins with the uniform inflow conditions, which serve as a baseline for the subsequent sheared cases. Figure 2 illustrates the normalized time-averaged flow fields of the streamwise component of the velocity, for three representative advance ratio $\boldsymbol{J} = 0.4$, 0.5 and 0.6. These baseline cases depict the classic propeller slipstream structure, where the influence of $\boldsymbol{J}$ on the flow acceleration behind the rotor and the subsequent wake development is clearly visible. In particular, as the advance ratio increases, we notice a lower slipstream contraction, as expected.

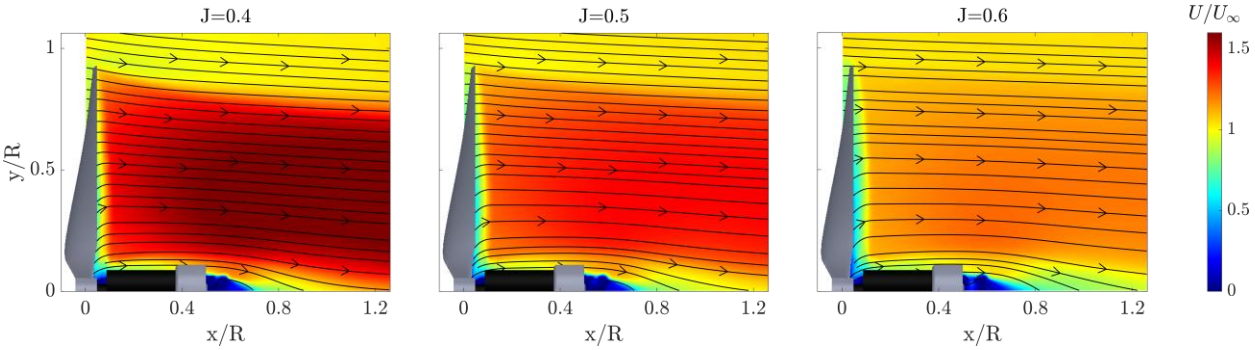


Figure 2: Time-averaged flow fields of the normalized streamwise velocity component. Cases of uniform inflow at J= 0.4, 0.5 and 0.6.

When introducing a sheared inflow, clear modifications in the wake topology are observed. This effect is highlighted in Figure 3, which displays the normalized out-of-plane vorticity (Ω_z) contours for the $J = 0.4$ case. The figure contrasts the baseline uniform inflow (a) against the four increasing shear rates, SR_1 to SR_4 (b-e). Two primary observations emerge. First, a progressive reduction in the overall vorticity magnitude is observed as the inflow shear rate increases. This distortion is an inevitable consequence of the inflow condition: a sheared flow imposes a non-uniform velocity U across the propeller disk. This, in turn, locally modifies the advance J and thus the aerodynamic loading on different sections of the blade, leading to an asymmetric and deformed wake structure.

Materials Research Proceedings 69 (2026) 707-712 https://doi.org/10.21741/9781644904251-125

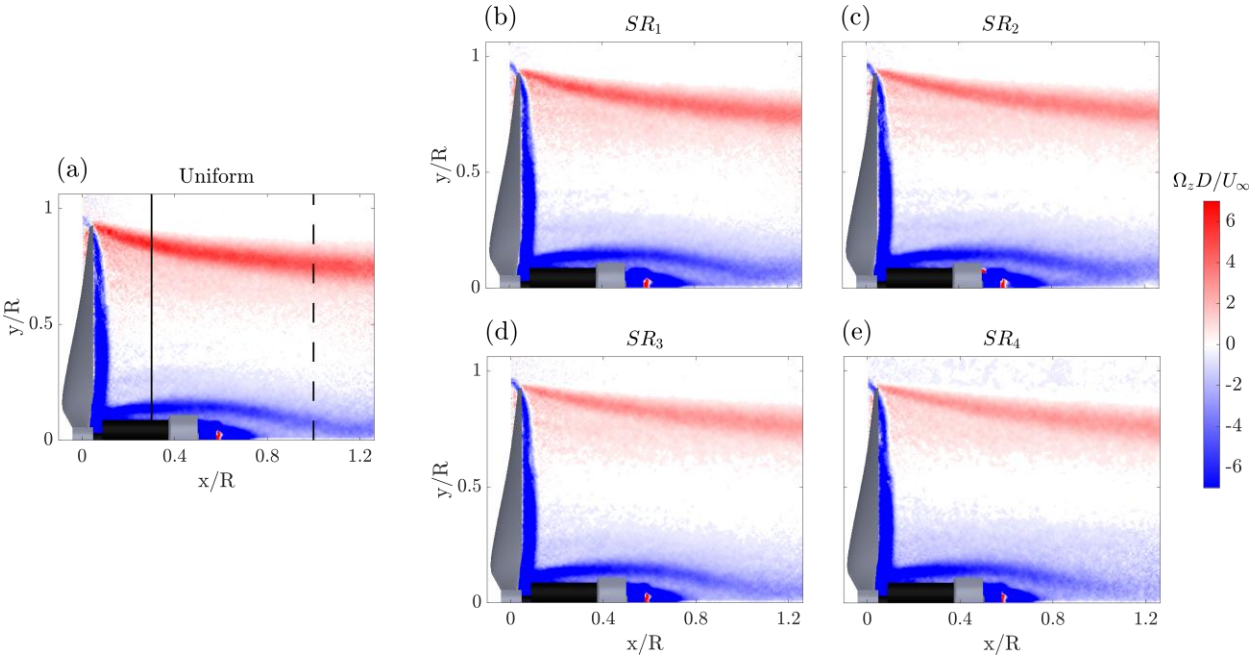


Figure 3: Time-averaged flow fields of the normalized out-of-plane vorticity $\boldsymbol{\Omega_z}$. Cases at $\boldsymbol{J = 0.4}$. (a) Uniform inflow. (b-e) Increasing sheared inflow from $\boldsymbol{SR_1}$ to $\boldsymbol{SR_4}$. The vertical solid ($\boldsymbol{x/R = 0.3}$) and dashed ($\boldsymbol{x/R = 1}$) lines in (a) indicate the reference stations selected for subsequent analysis.

To provide a more quantitative observation, Figure 4 shows the radial profiles of the normalized vorticity at the two reference stations identified by the two black lines in Figure 3(a). The results are presented for two advance ratios, $\boldsymbol{J} = 0.4$ and $\boldsymbol{J} = 0.6$. Within each plot, the solid lines refer to the station closer to the blades ($\boldsymbol{x/R} = 0.3$), while the dashed lines represent the station further downstream ($\boldsymbol{x/R} = 1$). The different colors distinguish the uniform inflow case from the four sheared conditions ($\boldsymbol{SR_1 - SR_4}$). Analyzing the near-wake station at $\boldsymbol{x/R} = 0.3$, two distinct peaks of opposite sign are evident. The negative peak at lower $\boldsymbol{y/R}$ corresponds to the mean trace of the hub vortices, which roll up near the motor, while the positive peak at higher$\boldsymbol{y/R}$ marks the mean trace of the tip vortices detaching from the blade tips and evolving along the wake. Focusing on this positive peak, it is clear that as the inflow shear rate increases, its intensity progressively decreases. Moreover, the location of the peak shifts at higher radial positions ($\boldsymbol{y/R}$), indicating an expansion of the streamtube in the analyzed region. By comparing the two plots, it is also evident that this combined effect (reduction in intensity and outward shift) is more pronounced at the lower advance ratio.

To further investigate the wake's turbulent characteristics, the velocity field is decomposed into its mean (U) and fluctuating (u') components using Reynolds decomposition. From the fluctuating parts, the Turbulent Kinetic Energy is computed as $TKE = {}^{1}/_{2}\left(\overline{u'^2} + \overline{v'^2}\right)$, considering only the measured components of the velocity fluctuations.

Materials Research Proceedings 69 (2026) 707-712 https://doi.org/10.21741/9781644904251-125

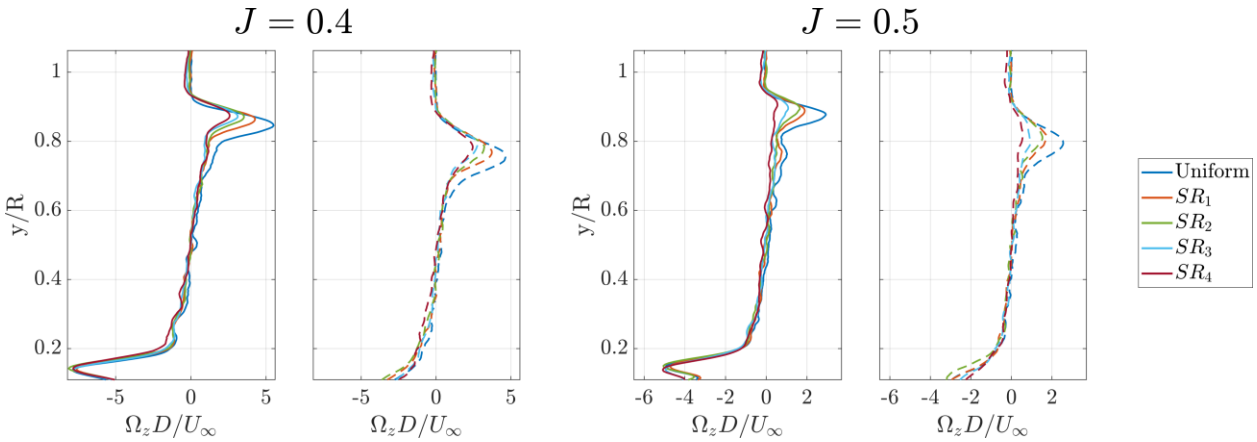


Figure 4: Radial profiles of normalized out-of-plane vorticity ($\boldsymbol{\Omega_z}$) for $\boldsymbol{J = 0.4}$ (left) and $\boldsymbol{J = 0.5}$ (right). Solid lines correspond to the near-wake station ($\boldsymbol{x/R = 0.3}$) and dashed lines to the far-wake station ($\boldsymbol{x/R = 1}$).

Figure 5 shows the radial profiles of the TKE at the same downstream stations ($x/R = 0.3$ and $x/R = 1$) and for the same advance ratios ($J = 0.4$ and $J = 0.5$) analyzed for the vorticity. A clear distinction emerges between the inflow conditions. For the uniform inflow cases, the TKE is highly concentrated, showing a sharp peak co-located with the mean tip vortex trace. This indicates that turbulence generation is primarily localized in that region. Conversely, in the presence of sheared inflow, the TKE is more diffused and spread out across the entire radial extent of the wake and is less localized in the tip region, suggesting that the incoming shear promotes a more widespread turbulence production and mixing.

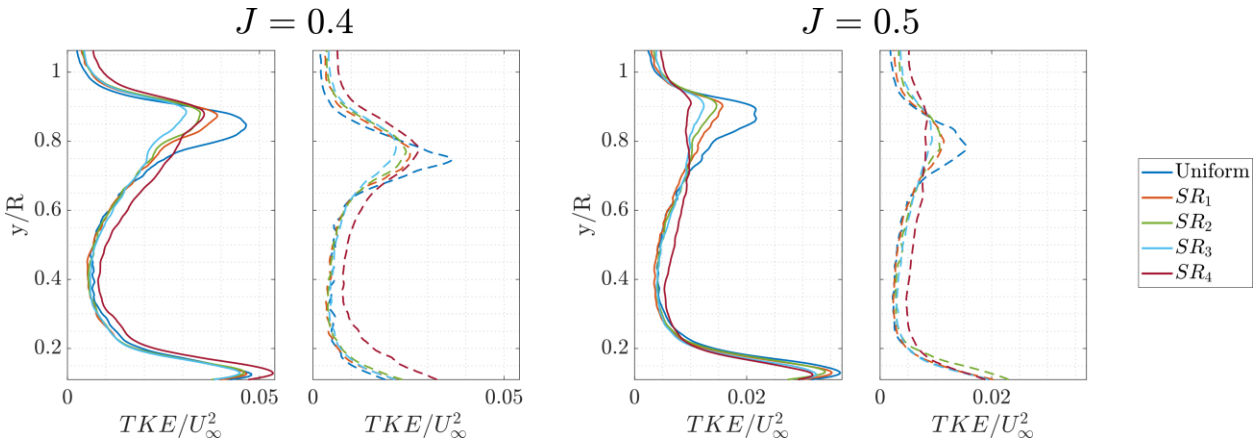


Figure 5: Radial profiles of normalized TKE for $\boldsymbol{J = 0.4}$ (left) and $\boldsymbol{J = 0.5}$ (right). Solid lines correspond to the near-wake station ($\boldsymbol{x/R = 0.3}$) and dashed lines to the far-wake station ($\boldsymbol{x/R = 1}$).

Summary and outlooks

This study presented an experimental PIV analysis of a propeller wake under both uniform and controlled sheared inflow conditions. The uniform inflow cases served as a baseline, exhibiting the expected slipstream contraction which diminished with increasing advance ratio $\boldsymbol{J}$. The introduction of a linear sheared inflow was shown to fundamentally alter the wake topology. The local changing of the operating conditions creates an asymmetric development of the wake, characterized by a reduction in the mean tip vortex vorticity and a radial expansion of the streamtube in the region under investigation. These effects are more pronounced at lower advance

ratios. Furthermore, the turbulence characteristics were significantly modified: while the TKE is highly localized in the tip vortex core for uniform flow, it becomes broadly diffused across the wake under shear, indicating enhanced turbulent mixing.

These results confirm that even in the simplest conditions of a linearly sheared inflow, the wake evolution is clearly affected, highlighting the limitations of uniform-inflow assumptions for UAM applications.

Acknowledgments
This study was carried out within the MOST – Sustainable Mobility National Research Center and received funding from the European Union Next-GenerationEU (PIANO NAZIONALE DI RIPRESA E RESILIENZA (PNRR) – MISSIONE 4 COMPONENTE 2, INVESTIMENTO 1.4 – D.D. 1033 17/06/2022, CN00000023). This manuscript reflects only the authors' views and opinions, neither the European Union nor the European Commission can be considered responsible for them. SM was supported by a scholarship funded through the WINDED Scalability Project, (PIANO NAZIONALE DI RIPRESA E RESILIENZA (PNRR) – MISSIONE 4 COMPONENTE 2, INVESTIMENTO 1.4 – D.D. 1033 17/06/2022, CN00000023**).**

References

[1] Betti Sorbelli, F. (2024). UAV-Based Delivery Systems: A Systematic Review, Current Trends, and Research Challenges. ACM Journal of Autonomous Transportation Systems, 1(3), Article 12. https://doi.org/10.1145/3649224

[2] Zhang, C., Xie, S. & Qin, T., Aerodynamic Analysis of Small Propeller in Wind Field Using CFD, 4th International Conference on Sustainable Energy and Environmental Engineering (ICSEEE 2015), 2015. https://doi.org/10.2991/icseee-15.2016.148

[3] Park, S., Lee, S., Im, B., Lee, D. & Shin, S., Improvement of a multi-rotor UAV flight response simulation influenced by gust, Aerospace Science and Technology, 134, 108156, 2023. https://doi.org/10.1016/j.ast.2023.108156

[4] Cerny, M. & Breitsamter, C., Investigation of small-scale propellers under non-axial inflow conditions, Aerospace Science and Technology, 106, 106048, 2020. https://doi.org/10.1016/j.ast.2020.106048

[5] Noca, F., Bujard, T., Visvaratnam, G., Catry, G., & Bosson, N. (2021). Flow Profiling in a Windshaper for Testing Free-Flying Drones in Adverse Winds. HES-SO University of Applied Sciences and Arts Western Switzerland, and WindShape, Geneva, Switzerland. https://doi.org/10.2514/6.2021-2577

[6] Casalino, D., Grande, E., Romani, G., Ragni, D., & Avallone, F. (2021). Definition of a benchmark for low Reynolds number propeller aeroacoustics. Aerospace Science and Technology, 113, 106707. https://doi.org/10.1016/j.ast.2021.106707

[7] Paolillo, G. & Astarita, T., PaIRS-UniNa: a robust and accurate free tool for digital particle image velocimetry and optical camera calibration, 21st International Symposium on Application of Laser and Imaging Techniques to Fluid Mechanics, 2024. https://doi.org/10.55037/lxlaser.21st.120